Pergamon

Atmospheric Environment Vol. 29, No. 22, pp. 3235–3238, 1995

1352-2310/95 $9.50 + 0.00

1352–2310(95)00259–6

A METHOD FOR COMPUTING SINGLE TRAJECTORIES REPRESENTING BOUNDARY LAYER TRANSPORT

ANDREAS STOHL and GERHARD WOTAWA

Institute of Meteorology and Geophysics, University of Vienna Hohe Warte 38, A-1190 Wien, Austria

(*First received* 3 *November* 1994 *and in final form* 19 *June* 1995)

Abstract—For many purposes it is necessary to represent the transport of air pollutants by a single trajectory. Examples are models which simulate the physical and chemical processes within a box moving along a trajectory or the receptor-oriented statistical modelling of air pollutants. Especially within the planetary boundary layer strong vertical wind shear poses serious problems for describing transport processes with a single trajectory. This paper describes a new method for calculating boundary layer trajectories which uses a pollutant mass-weighted transport vector. For evaluating this vector it is assumed that the pollutant is evenly distributed within the mixed layer. During periods of reduced mixed layer depth (e.g. nighttime) a residual layer may form above the mixed layer and most of the pollutant is transported aloft. However, this residual layer transport is only of interest if the mixed layer height rises again and pollutants are fumigated back to ground-level. Thus, estimation of the most appropriate pollutant transport depth requires the knowledge of mixing heights along the whole trajectory from the starting point to the receptor point. As this information is not *a priori* available, an iterative scheme was developed which uses the mixing heights along a preliminary trajectory as an input for an improved guess of the final trajectory. Experiments have shown that this method converges very fast. The computation of a first guess trajectory with fixed transport depth and one iteration is sufficient.

Key word index: Trajectories, planetary boundary layer, transport of air pollutants.

1. INTRODUCTION

The calculation of trajectories is a widely used tool in the environmental sciences. As emissions of air pollutants mostly take place near ground level, the calculation of trajectories within the planetary boundary layer (PBL) is of special importance. Due to the mixing of air pollutants and the strong vertical shear of the horizontal wind, it is very difficult to describe PBL transport with a single trajectory. Only multiple-particle dispersion models can fully represent PBL transport processes. Unfortunately, for many applications the transport has to be approximated by a single trajectory. This is especially true for receptor-oriented statistical or physical–chemical modelling of the transport of air pollutants. Receptor-oriented statistical modelling is able to identify potential source regions of air pollutants (e.g. Cheng and Hopke, 1993; Stohl and Kromp-Kolb, 1994) and Lagrangian box models have successfully been applied in many studies of air pollution problems such as acid deposition (e.g. Eliassen and Saltbones, 1983) or ozone formation (e.g. De Leeuw *et al.*, 1990; Simpson, 1993). All these methods need single-particle trajectories as an input and it is crucial to provide trajectories that follow the actual path of the air pollutants as closely as possible.

2. METHOD AND RESULTS

Several studies have investigated the uncertainties of trajectories within the PBL (e.g. Haagenson *et al.*, 1987, 1990; McQueen and Draxler, 1994). Due to the presence of diabatic processes, the isentropic framework (Danielsen, 1961) does not work properly in the PBL. Constant level trajectories have widely been used, but three-dimensional trajectories might be more adequate, especially during the passage of frontal systems when vertical motions are important. However, in any case one has difficulties in defining the most appropriate height of the starting level of the trajectories which is dependent on the meteorological conditions. In addition, turbulent processes tend to redistribute pollutants continuously within the PBL. Therefore, a vertically integrated transport vector (VITV) has frequently been used to describe PBL transport (e.g. Artz *et al.*, 1985; Haagenson *et al.*, 1987, 1990). The VITV is defined as

$$\mathrm{VITV} = \frac{1}{(p_u - p_s)} \int_{p_s}^{p_u} \mathbf{v}\, \mathrm{d}p$$

with $\mathbf{v}$ being the horizontal wind vector, p_s the surface presssure and p_u the pressure at the height of the upper boundary (UB) of the transport layer. The

VITV describes the mass mean transport in the PBL and should yield the best-possible estimate for PBL transport. Haagenson *et al.* (1987), who compared isobaric, isentropic, isosigma, three-dimensional and VITV trajectories with tracer-derived trajectories, confirmed that the smallest separation between model and tracer trajectories occurs for the VITV technique. The same result was found by Haagenson *et al.* (1990) for the ANATEX data.

The major difficulty of the VITV technique is the definition of the UB. Many authors defined the UB as the height of the first non-surface-based inversion (e.g. Artz *et al.*, 1985). However, this approach is somewhat arbitrary and not entirely satisfying. The level of transport within a shallow nighttime PBL after a nighttime release of pollutants may, in particular, be overestimated. Thus, a new method will be presented here. It is based on the assumption that pollutants are emitted near ground level at the start of or along a trajectory and that one is mainly interested in the resulting ground-level concentrations at the end of the trajectory. For most applications this assumption is valid.

Due to turbulent processes, pollutants do not stay near ground level during the transport, but are mixed nearly instantaneously within the mixed layer. The mixing height itself, however, cannot be used as the UB, because subsequent to a daytime release of air pollutants the nighttime transport does not take place in the shallow mixed layer, but in a residual aged smog layer aloft. Thus, it is necessary to develop a scheme which takes this into account.

Given a time series $H_i, i = 1, n$ of the mixing heights along a trajectory of n equally spaced time steps, two rules are applied to determine the corresponding time series of the UBs $U_i, i = 1, n$ along the trajectory:

1. $U_i = \max(H_1, H_2, \ldots, H_i)\ \forall i | \max(H_{i+1}, H_{i+2}, \ldots, H_n) \geqslant \max(H_1, H_2, \ldots H_i)$;
2. $\forall i|$ not rule 1: $U_i = \max\{[H_j \cdot (k-i) + H_k \cdot (i-j)]/(k-j)\}$ for $j = 1, i$ and $k = i + 1, n$.

max means the maximum of the respective H_i, $\forall i|$ means "for all i". Rule 1 is applied in cases where transport occurs aloft and pollutants are subsequently fumigated back to the ground. For instance, if emissions occur in the afternoon during convective conditions, pollutants are probably carried up to more than 2000 m (Fig. 1). During the following night, the mixing height is much lower, probably in the range of 100 m. As pollutants are distributed up to 2000 m, the majority of the pollutants is transported aloft, above the mixed layer. Thus, the UB of the VITV should rather be 2000 m than 100 m. The following morning the mixing height rises again and the pollutants are incorporated into the mixed layer and fumigated to ground level.

Rule 2 applies when no subsequent fumigation occurs (Fig. 2). Using the example mentioned above, but assuming that the trajectory terminates in the early morning hours before convective mixing starts,

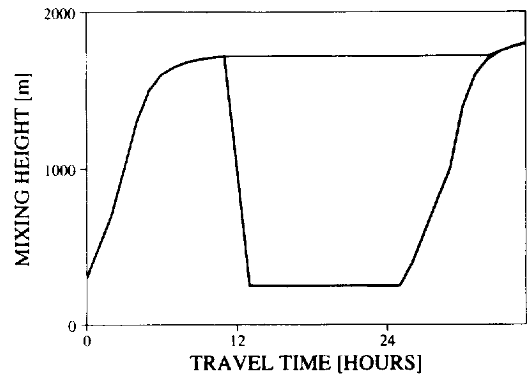

Fig. 1. Idealized example for the application of rule 1. The bold line represents the mixing height along the trajectory, the thin line is the UB of the VITV.

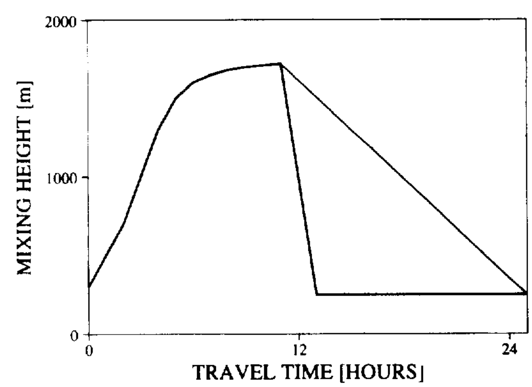

Fig. 2. Idealized example for the application of rule 2. For explanation see also Fig. 1.

the pollutants remain aloft and are not fumigated to the ground. As one is interested in the ground-level concentrations, in this case only the fraction of the pollutant which is transported within the shallow nighttime boundary layer is of interest and the UB should be in the range of 100 m. However, as some transport occurs even through the top of the PBL (especially for transport over several days), a linear decrease of the UB is assumed instead of a rapid change. Figure 3 shows an example of a multiday transport, where both rules are applied along the trajectory. Difficulties with this method can be expected in cases of strong vertical motions, either due to the passage of frontal systems or to cloud venting. However, especially in the latter case all types of trajectories will give questionable results.

The major problem with this approach is that during the computation of a forward trajectory one has no *a priori* knowledge of the subsequent mixing heights, whereas for backward trajectories one has no information about aged smog layers aloft. This problem has to be solved iteratively. One starts by calculating a trajectory with a constant UB (here 500 m);

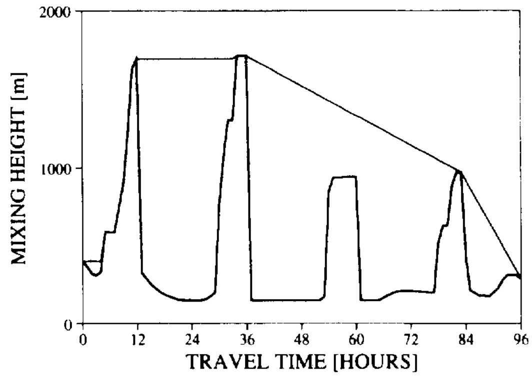

Fig. 3. Example for a multiday transport. For explanation see also Fig. 1.

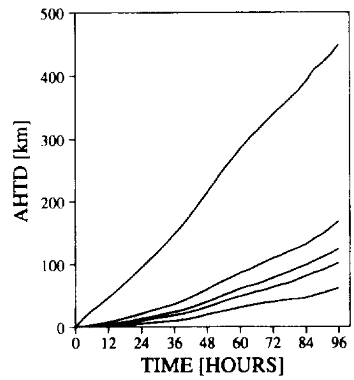

Fig. 4. The AHTD between the reference trajectories (sixth iteration) and the first five iterations as a function of travel time. The uppermost curve is for the first-guess trajectories and curves below are for subsequent iterations.

given this first guess trajectory and the mixing heights along its path, the UBs for each time step are determined from rules 1 and 2 and the computation of the trajectory is repeated with the new UB time series. Subsequent iterations improve the quality of the trajectory and the procedure may be terminated if the difference between trajectories of two subsequent iterations is below a certain threshold.

The convergence of the method described above was tested with the FLEXTRA trajectory model which is described in detail by Stohl *et al.* (1995). In this study FLEXTRA was based on model level analyses from the European Centre for Medium Range Weather Forecasts (ECMWF). These data have a horizontal resolution of 0.5° and a temporal resolution of 3 h; 14 levels up to approximately 4000 m above ground were used. The FLEXTRA model uses a flexible integration time step Δt which satisfies the Courant–Friedrichs–Lewy criterion $\Delta t = C\,\Delta x_i/u_i$, with $C < 1$, Δx_i being the grid distance in the ith direction and u_i the ith component of the wind speed. The integration scheme originally described by Pettersen (1940) is used. Convective mixing heights were calculated from ECMWF data by applying a procedure described by Beljaars and Betts (1992). Under stable conditions, mixing heights were derived from ECMWF friction velocity data following Holtslag *et al.* (1990).

Ninety six hours back trajectories for three starting positions were calculated in three-hourly intervals for the months April, July and December 1993. These months represent seasons of the year with different stream patterns and mixing heights. The total number of trajectories was 2040. Six iterations of the above-described procedure were carried out and the trajectories of the last iteration were used as a reference for a comparison with the other trajectories. For this purpose an absolute horizontal transport deviation,

$$\mathrm{AHTD}(t) = \frac{1}{N}\sum_{n=1}^{N}\sqrt{[x_a^n(t) - x_b^n(t)]^2 + [y_a^n(t) - y_b^n(t)]^2}$$

was defined in accordance with Kuo *et al.* (1985) and Rolph and Draxler (1990), where N is the total number of trajectories, (x_a, y_a) are the locations of the reference trajectories and (x_b, y_b) the locations of the trajectories for a given iteration at travel time t. Figure 4 presents the development of the AHTD with travel time. One can see that the AHTD is very large between the first guess and the sixth iteration (450 km after 96 h), but is reduced significantly for all subsequent iterations (below 168 km after 96 h). The factor of this reduction is much more pronounced for shorter travel times than for longer ones. For instance, the AHTD after 24 h is reduced from 79 km for the first guess trajectory to 18 km for the second and 4 km for the fifth iteration. The AHTDs after 96 h travel time varied by less than 20% for the three starting locations examined. Comparisons of results with initial UBs of 500 and 1000 m showed that the selection of the initial UB is of importance for the number of iterations needed to fulfil a specific convergence criterion (convergence for the 1000 m case was slower), but that the final solution does not depend on the choice of the initial UB.

It would be interesting to use data from tracer experiments for a validation of the VITV technique. Unfortunately, such data are not available to us. However, Stohl (1995) developed a method of trajectory statistics and applied it to determine source areas of particulate sulfate in Europe. For this work he used VITV trajectories and successfully identified source areas of sulfate which were in good agreement with an emission inventory. Computations with three-dimensional and especially constant-level trajectories were less successful in determining these source areas. This is an indication that the VITV technique is superior to the other types of trajectories.

3. SUMMARY AND CONCLUSIONS

A new method for computing single trajectories representing boundary layer transport was presented.

A vertically integrated transport vector was used and its upper boundary was determined from the time series of the mixing heights along the trajectory to approximate a pollutant mass weighted transport vector. The procedure requires an iterative computation of trajectories and mixing heights. Mixing heights along a trajectory from a first guess model run with constant transport height are used for an initialization of the iterative scheme. Subsequent iterations improve the accuracy of the trajectories. However, it can be seen from Fig. 4 that after the computation of the first guess trajectory a single iteration yields a sufficient accuracy in respect to other uncertainties of trajectory computations. This seems to be an affordable computational expense once the necessary input data are available. The final result was found to be independent of the choice of the initial transport height. In the future, comparisons with tracer-derived trajectories will allow an assessment of the actual improvement in accuracy with these PBL trajectories.

REFERENCES

Artz R., Pielke R. A. and Galloway J. (1985) Comparison of the ARL/ATAD constant level and the NCAR isentropic trajectory analyses for selected case studies. *Atmospheric Environment* **19**, 47–63.

Beljaars A. C. M. and Betts A. K. (1992) Validation of the boundary layer representation in the ECMWF model. *Seminar Proc. Validation of Models Over Europe*, Vol. II, 7–11 September 1992, Reading.

Cheng M.-D. and Hopke P. K. (1993) A receptor-oriented methodology for determining source regions of particulate sulfate observed at Dorset, Ontario. *J. geophys. Res.* **98**, 16,839–16,849.

Danielsen E. F. (1961) Trajectories: Isobaric, isentropic and actual. *J. Met.* **18**, 479–486.

De Leeuw F. A. A. M., Van Rheineck Leyssius H. J. and Builtjes P. J. H. (1990) Calculation of long term averaged ground level ozone concentrations. *Atmospheric Environment* **24A**, 185–193.

Eliassen A. and Saltbones J. (1983) Modelling of long-range transport of sulphur over Europe: a two-year model run and some model experiments. *Atmospheric Environment* **17**, 1457–1473.

Haagenson P. L., Kuo Y.-H., Skumanich M. and Seaman N. L. (1987) Tracer verification of trajectory models. *J. Clim. appl. Met.* **26**, 410–426.

Haagenson P. L., Gao K. and Kuo Y.-H. (1990) Evaluation of meteorological analyses, simulations, and long-range transport calculations using ANATEX surface tracer data. *J. appl. Met.* **29**, 1268–1284.

Holtslag A. A. M., De Bruijn E. I. F. and Pan H. L. (1990) A high resolution air mass transformation model for short range weather forecasting. *Mon. Weath. Rev.* **118**, 1561–1575.

Kuo Y.-H., Skumanich M., Haagenson P. L. and Chang J. S. (1985) The accuracy of trajectory models as revealed by the observing system simulation experiments. *Mon. Weath. Rev.* **113**, 1852–1867.

McQueen J. T. and Draxler R. R. (1994) Evaluation of model back trajectories of the Kuwait oil fires smoke plume using digital satellite data. *Atmospheric Environment* **28**, 2159–2174.

Petterssen S. (1940) *Weather Analysis and Forecasting*. McGraw-Hill, New York.

Rolph G. D. and Draxler R. R. (1990) Sensitivity of three-dimensional trajectories to the spatial and temporal densities of the wind field. *J. appl. Met.* **29**, 1043–1054.

Simpson D. (1993) Photochemical model calculations over Europe for two extended summer periods: 1985 and 1989. Model results and comparison with observations. *Atmospheric Environment* **27A**, 921–943.

Stohl A. (1995) Trajectory statistics—a new method to establish source-receptor relationships of air pollutants and its application to the transport of particulate sulfate in Europe. *Atmospheric Environment* (accepted).

Stohl A. and Kromp-Kolb H. (1994) Origin of ozone in Vienna and surroundings, Austria. *Atmospheric Environment* **28**, 1255–1266.

Stohl A., Wotawa G., Seiberg P. and Kromp-Kolb H. (1994) Interpolation errors in wind fields as a function of spatial and temporal resolution and their impact on different types of kinematic trajectories. *J. appl. Met.* **34**, 2149–2165.